JOURNAL OF MATERIALS SCIENCE 31 (1996) 6015–6024

Effect of cold drawing on environmentally assisted cracking of cold-drawn steel

J. TORIBIO
Department of Materials Science, University of La Coruña, ETSI Caminos, Campus de Elviña, 15192 La Coruña, Spain

A. M. LANCHA
CIEMAT, Ciudad Universitaria, 28040 Madrid, Spain

The fracture behaviour in air and aggressive environments of two eutectoid steels in the forms of hot-rolled bar and cold drawn wire has been compared to elucidate the consequences of cold drawing on their susceptibility to environmentally assisted cracking (EAC) in aqueous environments. Cold drawing produces a microstructural effect on the material: a preferential orientation of the pearlite lamellae aligned parallel to the cold-drawing direction, resulting in anisotropic properties with regard to fracture behaviour in air and aggressive environments. The main consequence is the change in crack-propagation direction approaching that of the wire axis (cold-drawing direction or main average orientation of the pearlite lamellae) and producing a mixed-mode state. The results reported provide insight into the macro- and micro-mechanical effects of cold drawing on the fracture and EAC-behaviour of eutectoid pearlitic steels.

1. Introduction

High-strength prestressing steels, usually in the form of cold-drawn eutectoid steel wires, are widely used in prestressed concrete structures, because after cold drawing their yield strength is high enough to guarantee normal service in the elastic range. However, prestressing steel wires are usually applied in harsh environments, and can suffer stress corrosion cracking and/or hydrogen embrittlement, i.e. environmentally assisted cracking (EAC) in several forms, from pure stress corrosion cracking to hydrogen embrittlement phenomena [1].

Cathodic protection methods are commonly used to avoid corrosion damage, and the risk of hydrogen embrittlement by overprotection has been profusely studied in high-strength prestressing steels under monotonic [2–4] and cyclic loading [5–6], showing that applying a cathodic overpotential to protect the steel against stress corrosion cracking results in an increasing risk of hydrogen embrittlement in the material. Galvanizing is other procedure frequently proposed to protect prestressing steels against stress corrosion cracking while inhibiting hydrogen embrittlement [7].

Works on the EAC of cold-drawn prestressing steels in the form of wires and tendons can be found in the technical literature. The general study reported by Parkins *et al.* [1] deals with environment-sensitive cracking of prestressing steels in the form of initially smooth, notched and pre-cracked samples, analysing the different cracking regimes dependent on the electrochemical potential. Cherry and Price [8] and Sarafianos [9] studied the EAC of prestressing steel wires in the absence of notches or pre-cracks, and described a kind of fracture by longitudinal splitting, whose orientation approaches the wire axis direction owing to the highly anisotropic nature of the prestressing steel after cold drawing. This was called flat-bottomed or layer-type corrosion damage [8] or exfoliation corrosion [9].

Specific works on hydrogen embrittlement of cold drawn steel can be found elsewhere [10–12]. Langstaff *et al.* [10] studied hydrogen-induced delayed failure of smooth wires, and concluded that cold drawing increases the resistance of the wire to hydrogen-induced delayed failure, but on the other hand, it promotes the formation of internal fissures and voids in the material, thus limiting the beneficial influence. Price *et al.* [11] studied the role of notches in the hydrogen embrittlement of steel prestressing tendons, and described the flat-bottomed or layer-type cracking, mentioned above, by longitudinal splitting or delamination. Toribio and Lancha [12] analysed the effect of cold drawing on the macroscopic susceptibility to hydrogen embrittlement of prestressing steel, and compared the behaviour of the material in the form of hot-rolled bar and cold-drawn wire, and concluded that the highest strength steel is the most susceptible to hydrogen embrittlement. A model to explain this effect was also formulated.

This paper analyses the influence of cold drawing on the fracture and EAC behaviour of a high-strength eutectoid steel used for civil engineering purposes in the prestressed concrete technique. Emphasis is placed

0022–2461

on the consequences of manufacturing (cold-drawing process) on environmentally assisted cracking of the steel from the macroscopic and microscopic points of view.

2. Materials: effect of cold drawing

A high-strength eutectoid steel supplied from commercial stock by EMESA (La Coruña, Spain) was used in this work. It is the steel used in the production of cold-drawn wire for prestressed concrete. The chemical composition is given in Table I. This steel was tested in two conditions: firstly, as hot-rolled patented cylindrical bars of 12 mm diameter, and secondly, as a commercial 7 mm diameter cold-drawn prestressing wire obtained from the bar. The prior hot-rolled steel presents a coarse pearlitic microstructure (austenite grain size 50–60 μm, pearlite interlamellar spacing 0.3 μm). After rolling, the 12 mm diameter bar was patented by cooling from the austenitic condition in a molten lead bath to produce fine pearlite (interlameller spacing around 0.1 μm). The wire was obtained by cold drawing this bar in six passes, to achieve an overall reduction of 66%, and finally a stress-relieving process was supplied involving exposure to about 400 °C for a few seconds.

The mechanical properties of both the bar and the wire are presented in Table II, and Fig. 1 shows the stress–strain curves of these materials. The fracture toughness, K_{IC}, was determined using cylindrical pre-cracked specimens obtained from the bar and the wire (for which the plane strain condition is achieved at the inner points of the crack [13]) together with an expression for the maximum stress intensity factor at the deepest point of the crack (assumed semi-elliptical) calculated by using the finite element method (FEM) combined with a virtual crack extension technique [14].

As described above, the microstructure of both steels consists of fine pearlite with an interlamellar spacing of 0.1 μm [15], measured according to the procedure described elsewhere [16]. Fig. 2 shows the microstructure of both the hot-rolled patented bar and the cold-drawn wire in transverse and longitudinal cross-sections. While the hot-rolled bar has a randomly-oriented microstructure in both transverse and longitudinal sections (Fig. 2a and c), the cold-drawn wire presents a randomly oriented appearance in the transverse cross-section (Fig. 2b), but a marked orientation in the longitudinal cross-section (Fig. 2d), which implies an effect of manufacturing on the resulting microstructure. Thus the cold-drawn wire presents features consisting mainly of alternate lamellae of ferrite and cementite aligned parallel or quasi-parallel to the wire axis or cold-drawing direction, which agrees with previous observations on similar microstructures [17–19]. The main phenomenological consequence will be a highly anisotropic behaviour of the material in both fracture in air and EAC.

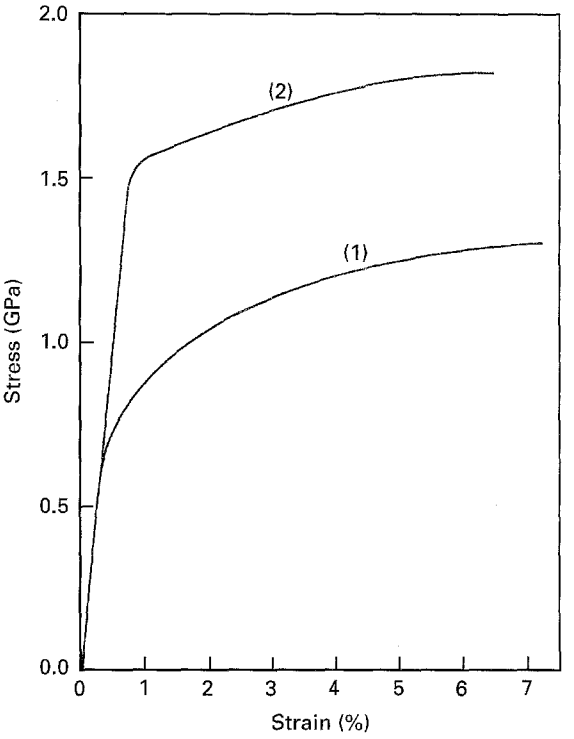

Figure 1 Stress–strain curves of the two steels: (1) hot-rolled, (2) cold-drawn.

TABLE I Chemical composition (wt %) of the steel

C	Mn	Si	P	S	Cr	Ni	Mo
0.74	0.70	0.20	0.016	0.023	0.01	0.01	0.001

3. Fracture in air

To characterize the basic fracture micromechanics of the two analysed steels in the absence of environmentally assisted processes (i.e. in an inert environment), smooth and pre-cracked samples of both steels were fractured in air, in order to elucidate also the influence of stress concentrations produced by cracks or sharp notches on the microscopic modes of fracture. Pre-cracked specimens were transversely pre-cracked rods, as shown in Fig. 3, and they also were used for the tests under aggressive environments, as described later. Results in the form of scanning

TABLE II Mechanical properties of the bar and the wire

Steel	Young's modulus (GPa)	Yield strength (MPa)	UTS (MPa)	Elongation under UTS (%)	Reduction of area (%)	Fracture toughness ($MPa\,m^{1/2}$)
1. Hot-rolled bar	195	725	1300	8.0	30	53
2. Cold-drawn wire	190	1500	1830	5.8	37	84

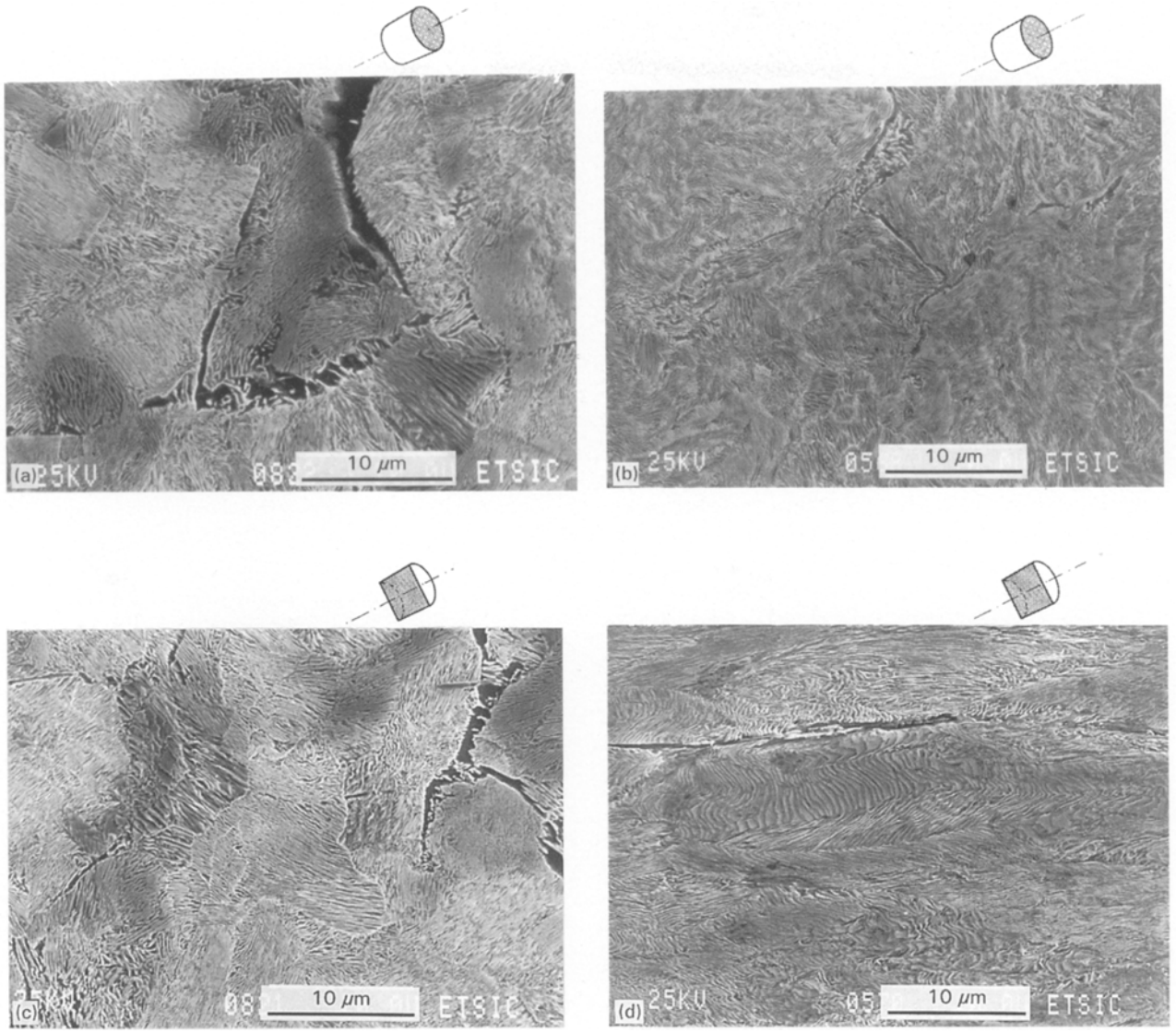

Figure 2 Microstructure of the (a, c) hot-rolled and (b, d) cold-drawn steels in (a, b) transverse and (c, d) longitudinal cross-sections.

electron micrographs are given in Fig. 4, together with a sketch showing the macroscopic shape and orientation of the fracture surface.

For the hot-rolled bar, the microscopic mode of fracture is micro-void coalescence (MVC) in the smooth sample (Fig. 4a, lowest level of triaxiality) and cleavage-like (C) in the pre-cracked one (Fig. 4c, highest level of triaxiality). In the cleavage-like topography, clear river patterns can be observed in the main direction of fracture propagation. For the cold-drawn wire, the microscopic mode of fracture is MVC in the smooth sample (Fig. 4b, lowest level of triaxiality), and MVC plus C in the pre-cracked one (Fig. 4d, highest level of triaxiality).

The MVC topography presents a dimpled appearance in both steels. However, the specific details of such a microscopic fracture mode in the hot-rolled bar are different from those appearing in the cold drawn wire (cf. Fig. 4a and b). The hot-rolled steel presents an MVC topography with numerous dimples closely spaced and a general fibrous aspect, whereas in the cold-drawn one, the density of dimples is lower, they are smaller than in the previous case and there are some areas with practically no hollows.

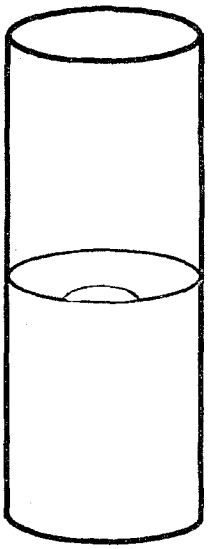

Figure 3 Pre-cracked specimens used in the experimental programme.

The stress concentration produced by the crack changes the micro-fracture mode from MVC to C in the hot-rolled bar, which is consistent with previous work demonstrating the role of triaxiality in the

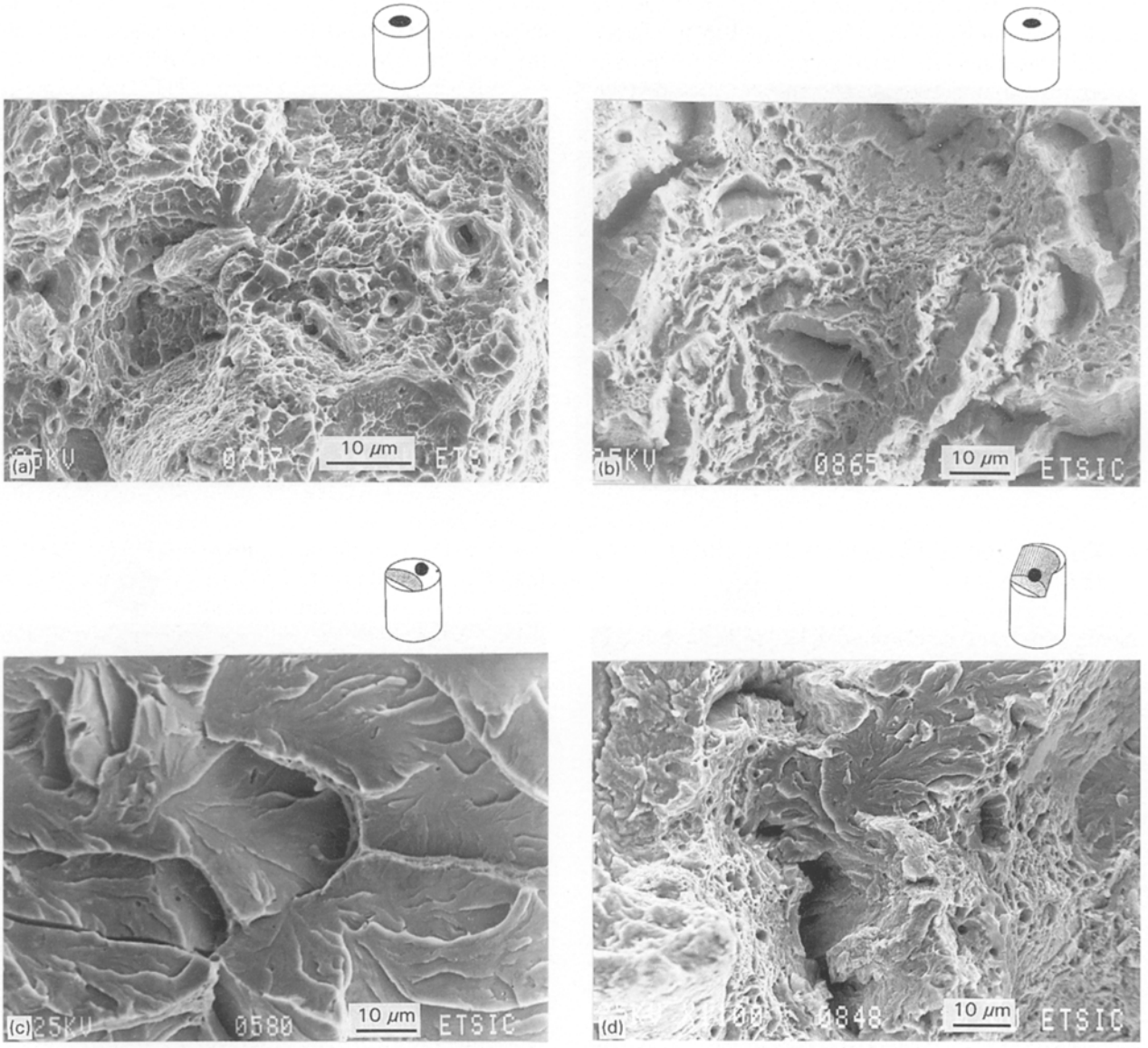

Figure 4 Microscopic modes of fracture in (a, b) smooth and (c, d) pre-cracked samples tested in an air environment: (a, c) hot-rolled, (b, d) cold drawn.

micro-fracture modes, and the trend towards a cleavage-like fracture for higher levels of triaxiality [20]. However, such a stress concentration does not really change the fracture mode in the cold-drawn wire, because it is still MVC. The only slight consequence is the appearance of some isolated cleavage facets which indicate a faster fracture than in the case of the smooth bar.

An important experimental fact is the change in crack-propagation direction in the pre-cracked sample of cold-drawn steel, tending to the wire axis direction, which represents a deviation angle of 70°–90° from that of the propagation throughout the initial plane of the crack (perpendicular to the wire axis). This is a consequence of the manufacturing process (cold drawing), consistent with the oriented appearance of the pearlite lamellae in the direction of the drawing axis, as shown in Fig. 2. It results in anisotropic fracture behaviour of the cold-drawn steel in air, a fact analysed in a previous work on the same kind of steel, also showing a change in the crack-propagation direction of about 70°–90° [21]. In this case the fracture toughness is a directional property of the material whose values depend on the particular propagation direction. As discussed in further sections, cold drawing and subsequent microstructure also produces a highly anisotropic EAC behaviour.

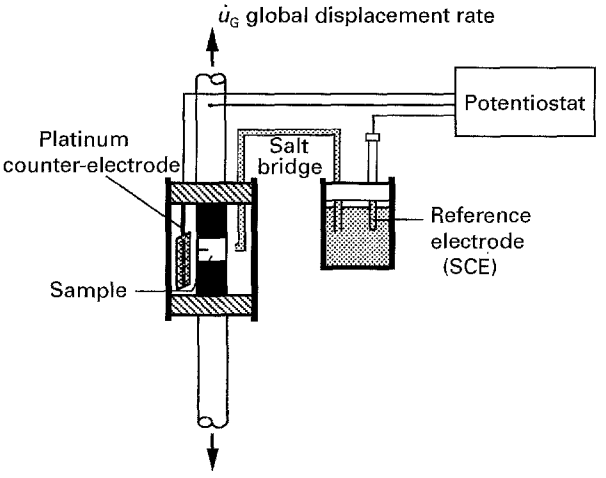

Figure 5 Experimental device used for the slow strain-rate tests (SSRT).

A doubt arises about the main microscopic fracture mode presumably obtained in pre-cracked specimens of cold-drawn steel fractured in air if the crack-propagation direction did not change but remained perpendicular to the wire axis, because the fibrous aspect of the fracture surface for angled cracks could be attributed to the coalescence of holes along minimum resistance paths, and perhaps cleavage propagation would appear if the crack grew along its initial direction. A simple model could explain this: considering the cold-drawn wire as formed by a set of high-resistance fibres aligned parallel to the direction of the wire axis and joined with low-resistance links in a direction perpendicular to that axis, a crack propagation consisting of separating the fibres (longitudinal splitting, delamination or exfoliation) would be much easier than in another for which the fibre had to be broken.

4. Environmentally assisted cracking (EAC) tests

The specimens used in the tests in aggressive environments were transversely pre-cracked rods, as shown in Fig. 3. The relationship between crack depth and cylinder diameter was the same for all specimens: $a/D = 0.3$; that is, $a = 4.0$ mm for the 12 mm diameter bars (hot-rolled), $a = 2.2$ mm for the 7 mm diameter wire (cold drawn). Samples were coated with an insulating lacquer except for a band about 1 mm wide on each side of the pre-crack.

Specimens were subjected to slow strain rate tests (SSRT) under axial loading in the direction of the wire axis. The applied displacement rate was 8.3×10^{-8} m s^{-1}, based on previous experience [1]. Testing was performed at room temperature (between 16 and 22 °C). The aggressive environment was an aqueous solution of 1 g l^{-1} $Ca(OH)_2$ plus 0.1 g l^{-1} NaCl to which HCl was added in varying amounts to adjust the pH value below the value of 12.5 for the base solution (pH = 12.5, 8.0 and 4.0 were chosen). All tests were carried out at a constant electrochemical potential by means of a potentiostat and a three-electrode assembly, as shown in Fig. 5. A broad range of electrochemical potentials was covered from the value $E = -100$ mV SCE (anodic) to the value $E = -1200$ mV SCE (cathodic).

Precracking of the samples was carried out by axial fatigue in the normal laboratory air environment. Various series of samples were prepared by using different fatigue loads during the last step of fatigue pre-cracking (just previous to the fracture test) in order to have control over this important experimental variable, which clearly influences the results in environmentally assisted cracking, as described in a previous paper [22]. The maximum stress intensity factor (SIF) levels in fatigue were $K_{max} = 0.28\ K_{IC}$, $0.45\ K_{IC}$, $0.60\ K_{IC}$ and $0.80\ K_{IC}$.

5. Macroscopic results of the EAC tests

The effects of the environmental conditions on fracture were quantified through the ratio of the failure load in the solution to the failure load in air. Fig. 6 includes all results for the hot-rolled bar and the cold-drawn wire and the three pH values, showing the well-known anodic and cathodic regimes of environment-sensitive cracking [1, 23]. The region of higher potentials is the anodic regime, and the associated EAC mechanism is localized anodic dissolution (LAD); the region of lower potentials is the cathodic regime, and the associated mechanism is hydrogen-assisted cracking (HAC).

A relevant K_{max} effect is observed due to compressive residual stresses in the vicinity of the crack tip during fatigue pre-cracking of the samples. This phenomenon has been discussed in previous works [12, 22, 24], the main conclusion being that high values of maximum SIF during fatigue pre-cracking, K_{max}, produce strong compressive residual stresses in the vicinity of the crack tip, thus delaying the hydrogen entry (in the case of HAC) or the metal dissolution (in the case of LAD).

For both steels, the susceptibility to HAC is greater than the susceptibility to LAD, i.e. the fracture load in the aggressive environment (compared with the same in air) is lower in the cathodic regime than in the anodic one. This means that pearlitic steels, in general, are more susceptible to HAC than to LAD, which is particularly true for the cold-drawn steel, nearly insensitive to LAD. This is a fundamental experimental result, because hydrogen could be present in the material not only at cathodic potentials but also at anodic ones, due to the local environment in the vicinity of the crack tip.

For anodic potentials, it can be observed that the results obtained for the cold-drawn wire are always above those of the hot-rolled bar. With regard to cathodic potentials, on the other hand, the consequence is not clear, and the behaviour of both steels is quite similar, the results of the cold-drawn wire being worse than those of the hot-rolled bar in some cases. Thus the cold-drawing process is beneficial against LAD processes, but not against HAC phenomena, which emphasizes the importance of HAC over LAD, not only because the former is more common (cf. previous paragraph), but also because its effect is more dangerous, especially for the final product, i.e. the cold-drawn wire to be used in prestressed concrete for civil engineering purposes.

In the following section of this paper, analysis is focused on the effect of the manufacturing process (in the form of cold drawing) on microscopic modes of fracture of the material under cathodic and anodic regimes, and therefore only the results for an intermediate value of fatigue pre-cracking load ($K_{max} = 0.45\ K_{IC}$) are analysed, all micrographs referring to this value.

6. Fractographic analysis of the EAC tests

6.1. Cathodic regime (HAC)

The main results of the fractographic analysis for the cathodic regime (HAC) are presented in Fig. 7. Fig. 7a and b show general micrographs at the crack tip, while specific micrographs of higher magnification are shown in Fig. 7c–f, giving parts of the fracture surface

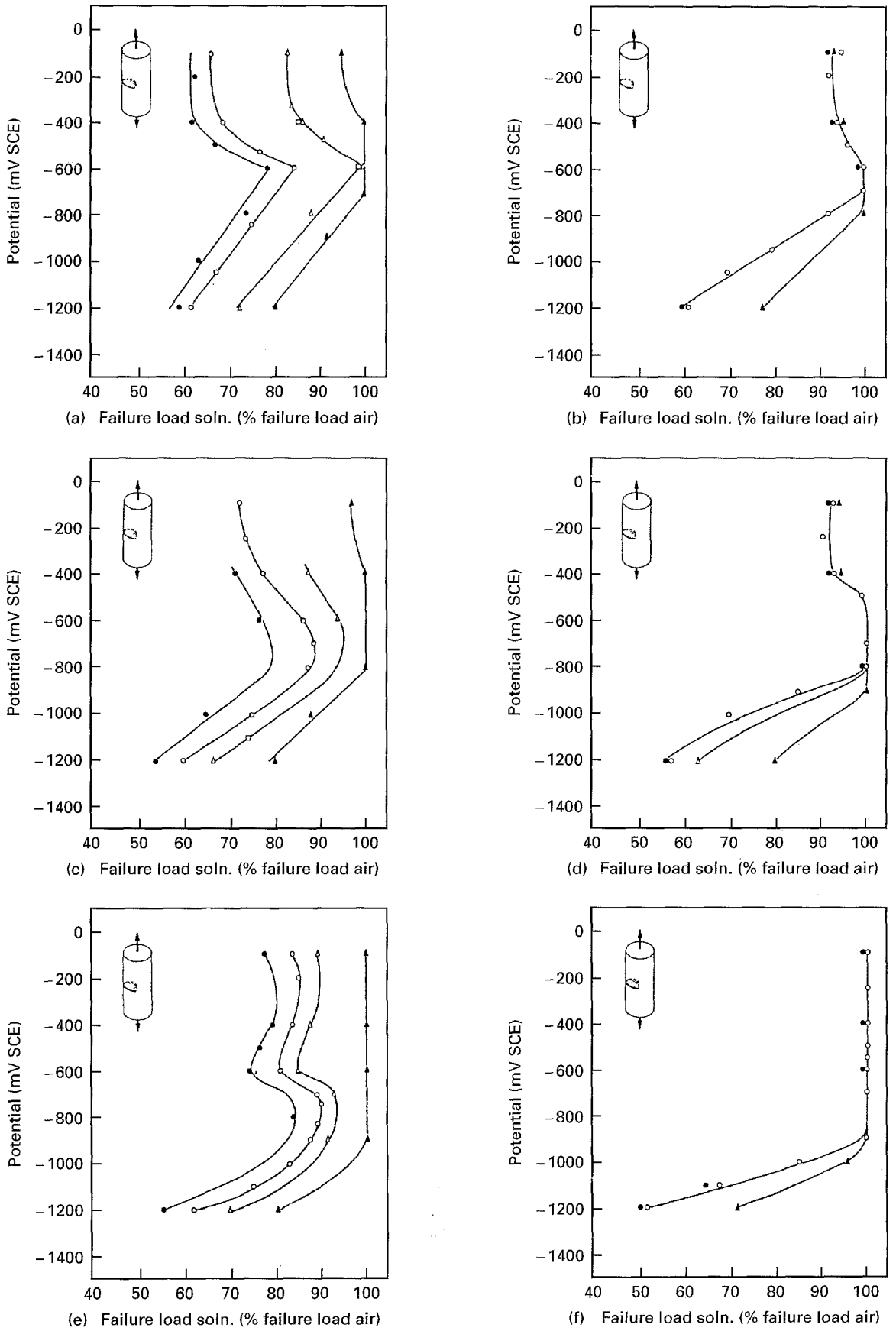

Figure 6 Experimental results of the SSRT. (a, c, e) Hot-rolled, (b, d, f) cold-drawn, at (a, b) pH 4.0, (c, d) pH 8.0, (e, f) pH 12.5. K_{max}: (●) 28% K_{IC}, (○) 45% K_{IC}, (▲) 80% K_{IC}. (a) (△) 65% K_{IC}, (□) 65% K_{IC} for $\phi = 7$ mm; (c) (△) 60% K_{IC}, (□) 60% K_{IC} for $\phi = 7$ mm; (d, e) (△) 60% K_{IC}.

corresponding to initiation (just at the crack tip) and propagation of fracture. As in the fracture in air, a sketch is given to show the macroscopic shape and orientation of the fracture surface in the wire.

Fracture of the hot-rolled specimens was macroscopically plane in direction perpendicular to the wire axis (mode I propagation). The microscopic fracture mode was the so-called tearing topography surface or

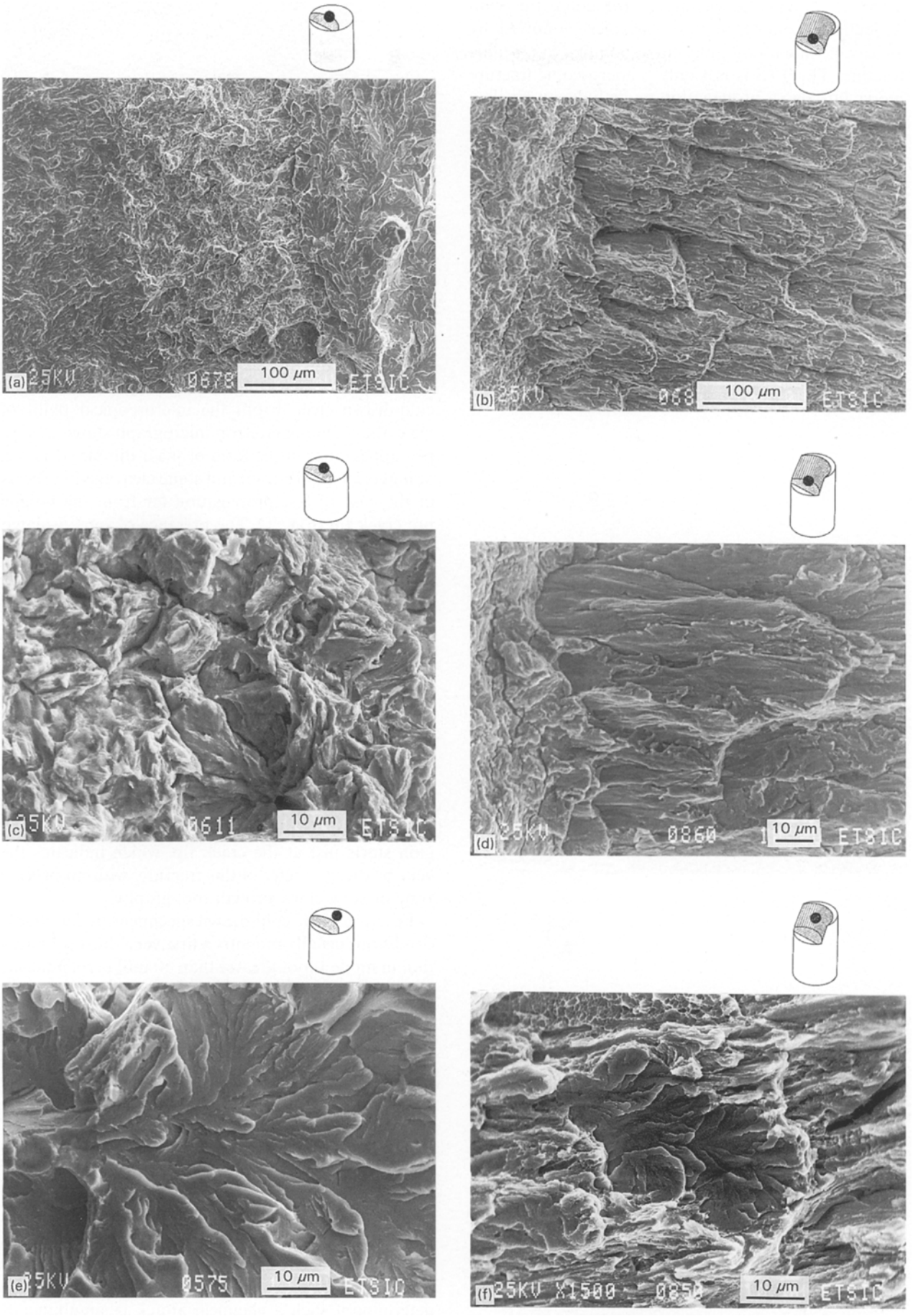

Figure 7 Microscopic modes of fracture in pre-cracked samples tested in the cathodic regime, i.e. under HAC conditions (pH = 12.5, $E = -1200$ mV SCE, $K_{max} = 0.45\ K_{IC}$) : (a) hot-rolled, general micrograph at the crack tip; (b) cold-drawn, general micrograph at the crack tip; (c) hot-rolled, TTS at the crack tip; (d) cold-drawn, shear dimples at the crack tip; (e) hot-rolled, cleavage-like propagation; (f) cold-drawn, mixed-mode propagation and cleavage-like facets.

TTS [25–27] in the vicinity of the crack tip (with a depth depending on test variables), followed by a cleavage-like topography corresponding to unstable fracture. The TTS is not only a microscopic fracture mode, but also a propagation mode linked with slow crack growth [25]. It resembles micro-cracking, micro-tearing or micro-damage [26], and is closely associated with hydrogen effects in pearlitic steel [27]. The general scanning electron micrograph in Fig. 7a shows the following sequence of cracking: fatigue pre-crack, TTS mode and cleavage-like propagation. Specific micrographs of the TTS and the cleavage-like micro-fracture modes (at higher magnification) are given in Fig. 7c and e, respectively.

Fracture of the cold-drawn specimens under cathodic conditions (Fig. 7b) presented a change in crack propagation direction, approaching the wire axis or cold-drawing direction and producing a macroscopically abrupt fracture surface and a mixed-mode effect, a consequence of the highly anisotropic nature of the cold-drawn steel. From the microscopical point of view, the scanning electron micrograph shows a stepped appearance in the form of shear dimples (Fig. 7d, at higher magnification) and some cleavage-like facets in the case of fast propagation far from the fatigue pre-crack tip (Fig. 7f). The presence of some isolated cleavage facets has a mechanical origin, as in the fracture of pre-cracked specimens in air (Fig. 4).

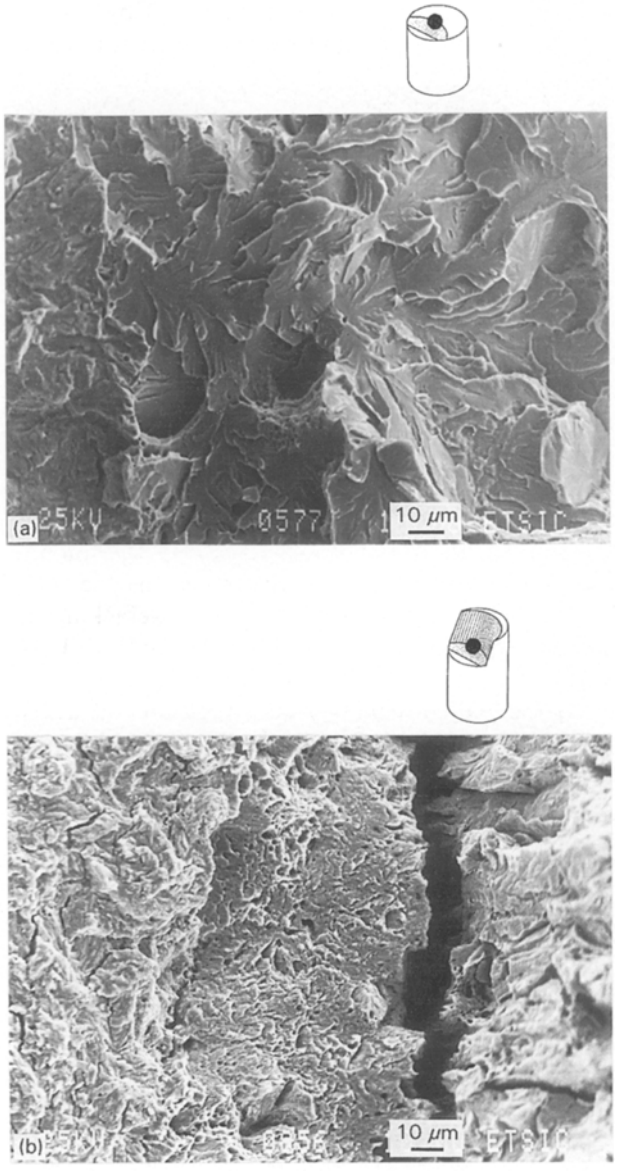

Figure 8 Microscopic modes of fracture in pre-cracked samples tested in the anodic regime, i.e. under LAD conditions (pH = 4.0, $E = -400$ mV SCE, $K_{max} = 0.45\ K_{IC}$) : (a) hot-rolled, cleavage-like fracture at the crack tip; (b) cold-drawn, change of the propagation direction from mode I to mixed mode.

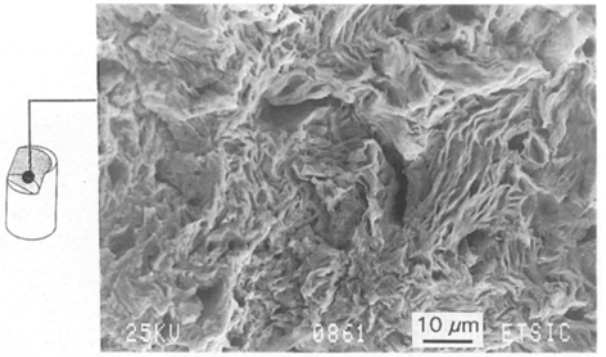

Figure 9 Scanning electron micrograph of a pre-cracked sample of cold-drawn steel tested in the anodic regime (LAD conditions) at pH = 8 and $E = -200$ mV SCE ($K_{max} = 0.45\ K_{IC}$) .

6.2. Anodic regime (LAD)

Fig. 8 shows the fractographic analysis for the anodic regime (LAD). Again fracture of the hot-rolled specimens was macroscopically plane in a direction perpendicular to the wire axis (mode I propagation). The scanning electron micrograph of this sample shows the typically brittle cleavage-like propagation after the fatigue pre-crack, with clear river patterns marking the fracture surface direction. This cleavage-like region starts just at the crack tip, which indicates the very brittle character of this fracture, with no process zone or slow crack-growth topography.

Fracture of the cold-drawn specimens under anodic conditions usually presents a first very short propagation in mode I (not greater than 50 μm) perpendicular to the wire axis, followed by a change in crack-propagation direction approaching that of cold drawing and producing the aforementioned mixed mode effect as a consequence of the anisotropic character of the cold-drawn steel. The microscopic appearance of such a surface is given in Fig. 8.

Fig. 9 shows a scanning electron micrograph of a pre-cracked sample of cold-drawn steel tested in the anodic regime (LAD conditions) at an even more anodic potential ($E = -200$ mV SCE). The fracture surface presents evidence of a strong attack with selected dissolution of the material. It is difficult to associate the evident chemical attack with a LAD mechanism at the crack tip, because it is impossible to determine if such a chemical attack is simultaneous with the LAD fracture process or is produced later, when the crack has grown further, as a consequence of the contact between the free metal surface (recently created) and the solution under anodic electrochemical potential.

6.3. Discussion

An in the case of the fracture in air, an important experimental fact is the change in crack-propagation direction tending to the wire axis or cold-drawing direction (main average orientation of the pearlite lamellae), with a deviation angle of 70°–90° from that of propagation along the initial plane of the crack (perpendicular to the wire axis). This is a consequence of the manufacturing process (cold drawing), consistent with the lamellar structure of the steel and the oriented appearance of the pearlite lamellae in the direction of the drawing axis (Fig. 2), resulting in a highly anisotropic EAC behaviour of the cold-drawn steel.

The anisotropic mode of failure of the cold-drawn wire may be viewed as longitudinal splitting [1, 8], exfoliation [9] or delamination [11], and with regard to EAC it has received names such as flat-bottomed or layer-type corrosion [8, 11] or exfoliation corrosion [9]. Other adequate names could be environmentally assisted splitting, exfoliation or delamination. The SEM appearance depends on the specific environmental conditions but, in general, it is more ductile and fibrous than in the case of mode I propagation for a given material–environment system.

From the fracture mechanics point of view, the afore-mentioned anisotropic behaviour results in a mixed-mode stress state in the vicinity of the crack tip, which represents an extremely difficult problem even in the framework of linear elastic fracture mechanics, with the additional difficulty of the environmentally assisted process. In this case, the solution of the problem requires the calculation of not only the critical stress or strain for fracture (in the form of fracture toughness, critical strain energy density or other parameter), but also the propagation angle according to the specific fracture criterion under consideration.

The change in crack-propagation direction produces two competing effects. On the one hand, it relaxes the stress concentration by producing a mixed-mode situation with lower K_I (zero value for a crack propagating in the direction of the wire axis). On the other hand, the new crack-growth path is that of minimum resistance to EAC, because this is precisely the reason for the change in the propagation angle, which makes the crack growth easier in both air and aggressive environments, as commented by Ali and Abbaschian [28] where it is said that cold working increases both the corrosion rate and the tendency to pitting.

With regard to the relationship between macroscopic (Fig. 6) and microscopic (Figs 7–9) effects on EAC behaviour of the steels, the cold drawn steel is shown to be more susceptible to HAC than to LAD. Furthermore, while cold-drawn steel is almost fully resistant to LAD, it is even more susceptible to HAC than the lower-strength hot-rolled steel. The reason could be the anisotropic effect with change in crack-propagation direction. In the case of LAD, the cold-drawn wire is able to undergo mode I cracking (Fig. 8b), thus making the crack grow by breaking tough links. For HAC, on the other hand, the crack changes its direction at the beginning of propagation, approaching a minimum resistance path (Fig. 7b and d).

The results of EAC confirm the damaging effects of cracks or notches (i.e. stress raisers) on the susceptibility of the material to EAC in several forms. This is especially important in hydrogen-assisted fracture [29], because hydrogen transport by diffusion is enhanced by the hydrostatic stress field in the vicinity of the notch and by the value of hydrostatic stress at the notch tip itself, as shown in a previous work [30].

7. Conclusions

1. Whereas the hot-rolled bar has a microstructure of randomly oriented pearlite lamellae, the cold-drawn wire presents an oriented microstructure consisting mainly of pearlite lamellae aligned quasi-parallel to the wire axis or cold-drawing direction, producing a highly anisotropic behaviour in both fracture in air and EAC.

2. The stress concentration generated by a crack changes the micro-fracture mode in an inert environment from MVC to C in the hot-rolled bar, but not in the cold-drawn wire, which breaks by MVC even when a crack is present, although in this case there is some evidence of isolated cleavage facets on the fracture surface.

3. Cold drawing produces longitudinal splitting, exfoliation or delamination in the pre-cracked samples fractured in air, with a change of 70°–90° in crack propagation direction tending to that of the wire axis (cold-drawing direction), which is also the main average orientation of pearlite lamellae, and represents a longitudinal crack path of minimum fracture toughness.

4. There is a beneficial effect of maximum fatigue pre-cracking load on ulterior EAC behaviour of the steel, in the form of an increase in the fracture load under an aggressive environment as the maximum SIF during the last stage of pre-cracking increases. This conclusion remains valid for both HAC and LAD.

5. Generally speaking, both the hot-rolled bar and the cold-drawn wire are more susceptible to HAC than to LAD. Indeed, the cold-drawn wire is almost fully resistant to LAD while it is strongly susceptible to HAC, even more than the hot rolled bar, whose behaviour under HAC and LAD conditions is similar.

6. The cold-drawing process is beneficial against LAD phenomena, because it increases clearly the fracture load in the anodic regime. However, the cold drawing is damaging against HAC processes, because it lowers dramatically the fracture load in a hydrogen environment (cathodic regime).

7. Under HAC conditions (cathodic regime) the pre-cracked hot-rolled bar fails in mode I by TTS followed by cleavage-like propagation, whereas the pre-cracked cold-drawn wire fails by shear dimples with some evidence of isolated cleavage facets, and the crack tends to the longitudinal orientation, producing a mixed-mode stress state.

8. Under LAD conditions (anodic regime) the pre-cracked hot-rolled bar fails in mode I by cleavage-like topography, whereas the pre-cracked cold-drawn wire presents a short mode I crack-growth path (50 μm), and an ulterior tendency to orientation parallel to the wire axis associated with a mixed-mode propagation.

9. Cold drawing produces environmentally assisted splitting, exfoliation or delamination in the pre-cracked samples fractured under an aggressive environment, which results in a mixed-mode stress state with a change in crack-propagation direction approaching that of pearlite lamellae, and represents a longitudinal crack path of minimum resistance to HAC or LAD.

10. The change in crack-propagation direction in the pre-cracked cold-drawn wires relaxes the stress concentration by producing a mixed-mode situation with lower K_I, but the new crack-growth path is that of minimum resistance to EAC. In the case of LAD, the cold-drawn wire is able to undergo mode I cracking, which improves its EAC behaviour.

Acknowledgements

The financial support of this work by the Spanish DGICYT (Grant UE94-001) and Xunta de Galicia (Grants XUGA 11801A93 and XUGA 11801B95) is gratefully acknowledged. The authors thank EMESA, La Coruña, Spain, for providing the steel used in the experimental programme.

References

1. R. N. PARKINS, M. ELICES, V. SACHEZ-GALVEZ and L. CABALLERO, *Corros. Sci.* **22** (1982) 379.
2. C. C. KUMRIA, W. H. HARTT and R. J. KESSLER, in "Proceedings of CORROSION/90", Las Vegas, Nevada, April 1990 (NACE, Houston TX, 1990) pp. 322/1–8.
3. W. H. HARTT, in "Corrosion of Reinforcement in Concrete", edited by C. L. Page, K. W. J. Treadaway and P. B. Bamforth (Elsevier, London, 1990) p. 515.
4. B. ISECKE and J. MIETZ, *Steel Res.* **64** (1993) 97.
5. J. CONGLETON, I. HUSSAIN and R. N. PARKINS, *Br. Corros. J.* **20** (1985) 5.
6. R. HAMANO, *J. Mater. Sci. Lett.* **8** (1989) 852.
7. Y. YAMAOKA, H. TSUBONO and M. KURAUCHI, *PCI J.* **33** (4) (1988) 146.
8. B. W. CHERRY and S. M. PRICE, *Corros. Sci.* **20** (1980) 1163.
9. N. SARAFIANOS, *J. Mater. Sci. Lett.* **8** (1989) 1486.
10. D. C. LANGSTAFF, G. MEYRICK and J. P. HIRTH, *Corros. NACE* **37** (1981) 429.
11. S. M. PRICE, P. G. WARDEN, T. S. CHIA, N. V. Y. SCARLETT and J. H. MAHONEY, *Mater. Forum* **16** (1992) 245.
12. J. TORIBIO and A. M. LANCHA, *Mater. Struct.* **26** (1993) 30.
13. M. A. ASTIZ, PhD thesis, Polytechnical University of Madrid (1976).
14. *Idem, Int. J. Fract.* **31** (1986) 105.
15. A. M. LANCHA, PhD thesis, Complutense University of Madrid (1987).
16. "ASM Metals Handbook", Vol. 9, "Metallography and Microstructures" (ASM, Metals Park, OH, 1985).
17. M. A. P. DEWEY and G. W. BRIERS, *J. Iron Steel Inst.* **204** (1966) 102.
18. J. D. EMBURY and R. M. FISHER, *Acta Metall.* **14** (1966) 147.
19. G. LANGFORD, *Metall. Trans.* **1** (1970) 465.
20. J. TORIBIO, A. M. LANCHA and M. ELICES, *Mater. Sci. Eng.* **A145** (1991) 167.
21. M. A. ASTIZ, A. VALIENTE, M. ELICES and H. D. BUI, in "Life Assessment of Dinamically Loaded Materials and Structures-ECF5", edited by L. Faria (EMAS, West Midlands, UK, 1984) p. 385.
22. J. TORIBIO, A. M. LANCHA and M. ELICES, *Corros. Sci.* **35** (1993) 521.
23. V. SANCHEZ-GALVEZ, L. CABALLERO and M. ELICES, ASTM STP **866** (American Society for Testing and Materials, Philadelphia, PA, 1985) p. 428.
24. J. TORIBIO and A. M. LANCHA, *J. Mater. Sci. Lett.* **14** (1995) 1204.
25. J. TORIBIO, A. M. LANCHA and M. ELICES, *Scripta Metall. Mater.* **25** (1991) 2239.
26. A. W. THOMPSON and J. C. CHESNUTT, *Metall. Trans.* **10A** (1979) 1193.
27. J. TORIBIO, A. M. LANCHA and M. ELICES, *ibid.* **23A** (1992) 1573.
28. S. I. ALI and G. J. ABBASCHIAN, *Br. Corros. J.* **12** (1977) 24.
29. A. W. THOMPSON, *Mater. Sci. Tech.* **1** (1985) 711.
30. J. TORIBIO, *J. Mater. Sci.* **28** (1993) 2289.

Received 3 January
and accepted 18 March 1996